

Individualized Dosing Algorithms and Therapeutic Monitoring for Antiepileptic Drugs

Sven C. van Dijkman¹, Sebastian G. Wicha², Meindert Danhof¹ and Oscar E. Della Pasqua^{3,4}

Pharmacokinetic (PK) models exist for most antiepileptic drugs (AEDs). Yet their use in clinical practice to assess interindividual differences and derive individualized doses has been limited. Here we show how model-based dosing algorithms can be used to ensure attainment of target exposure and improve treatment response in patients. Using simulations, different treatment scenarios were explored for 11 commonly used AEDs. For each drug, five scenarios were considered: 1) all patients receive the same dose. 2) Individual clearance (CL), as predicted by population PK models, is used to personalize treatment. 3–5) Individual CL, obtained by therapeutic drug monitoring (TDM) according to different sampling schemes, is used to personalize treatment. Attainment of steady-state target exposure was used as the performance criterion to rank each scenario. In contrast to current clinical guidelines, our results show that patient demographic and clinical characteristics should be used in conjunction with TDM to personalize the treatment of seizures.

Study Highlights

WHAT IS THE CURRENT KNOWLEDGE ON THE TOPIC?

✓ Population pharmacokinetic models are available for many antiepileptic drugs (AEDs), most of which allow the characterization of predictable (e.g., covariates) and random interindividual variability.

WHAT QUESTION DID THIS STUDY ADDRESS?

✓ Standard dosing recommendations and titration procedures have important limitations. A model-based algorithm is proposed for AED dose individualization, which may be of great benefit for patients who fail to respond to initial first-line therapy.

WHAT THIS STUDY ADDS TO OUR KNOWLEDGE

✓ AED dosing regimens based on typical population characteristics do not ensure attainment and maintenance of target exposure in patients. By contrast, model-based dosing algorithms result in significant reduction in the variability of AED levels at steady state.

HOW THIS MIGHT CHANGE CLINICAL PHARMACOLOGY OR TRANSLATIONAL SCIENCE

✓ Our approach shows how dosing algorithms can be implemented in the clinic to deliver personalized and individualized treatments. It also shows the advantages of integrating TDM with model-based platforms.

Epilepsy is a chronic neurological disease, manifesting as recurrent seizures. In spite of the efforts to identify novel, more effective antiepileptic drugs (AEDs), one-third of patients are not responsive to the first treatment. Sadly, a considerable proportion of these patients eventually also fail after transition to alternative or second-line treatment. Such interindividual variability in the response to AEDs is a consequence of multiple interacting factors, including differences in the pathophysiology, pharmacokinetics, pharmacodynamics, and genetic variation.^{1,2} It is therefore acknowledged that rational prescribing of AEDs requires not only an understanding of the seizure type and of the drugs' pharmacodynamic (PD) properties, but also careful consideration of the factors known to affect drug disposition.^{3,4} In fact, the impact of covariate factors on drug exposure and consequently on pharmacokinetic (PK) variability, efficacy, and tolerability profile of AEDs has been highlighted in a recent publication by our group.⁵ Our findings confirm the concerns raised by previous authors on the importance of accounting

for covariate factors, particularly in patients at the extreme range of age, such as infants and the elderly.^{6,7}

Given the impact of demographic, clinical, and genetic covariate factors, one important question that remains unaddressed is whether the lack of response and subsequently switching to alternative first-line AEDs (or combination therapy) can be potentially avoided by a more robust dosing rationale. Many AEDs show large PK variability, especially when drug–drug interactions occur during combination therapy.⁵ Nevertheless, despite the large number of investigations on the clinical pharmacokinetics of AEDs, limited attention has been given to the magnitude of such effects and their clinical implications. In most cases, covariate effects have been assessed as part of a population PK analysis, where the main objective is the characterization of the overall drug disposition properties and underlying sources of variability, rather than the optimization of the therapeutic intervention in a wider patient population.^{8,9}

¹Division of Pharmacology, Leiden Academic Centre for Drug Research, Leiden, The Netherlands; ²Department of Pharmaceutical Biosciences, Uppsala University, Uppsala, Sweden; ³Clinical Pharmacology Modelling & Simulation, GlaxoSmithKline, Uxbridge, UK; ⁴Clinical Pharmacology and Therapeutics, University College London, London, UK. Correspondence: O.E. Della Pasqua (o.dellapasqua@ucl.ac.uk)

Received 14 November 2016; accepted 20 June 2017; advance online publication 30 August 2017. doi:10.1002/cpt.777

From a clinical point of view, the use of titration procedures, without taking into account the underlying inter- and intraindividual variability in pharmacokinetics, conflate PK variability with that of pharmacodynamics and disease progression. Usually, treatment is started at a low dose, followed by up-titration until adequate efficacy or unacceptable side effects are reached. Therapeutic drug monitoring (TDM) is eventually considered when side effects are seen at a lower doses or inadequate efficacy is observed at a higher doses than expected. On the other hand, in some cases dosing regimens may be selected that aim at reaching steady-state concentrations (C_{ss}) within a predefined therapeutic range.^{10,11}

Based on the aforementioned, it becomes clear that current guidelines for the selection and titration of AEDs overlook the impact of the underlying variability in drug disposition. Even if only part of the PK variability can be explained by demographic covariates such as weight and age, dose adjustments can provide a concrete opportunity for optimizing AED therapy. Surprisingly, this contrasts with the fact that nomograms have had a place in the optimization of AED therapy since the early 1970s, especially for phenytoin, which shows large variability due to its nonlinear PK properties. Nomograms have, however, important limitations. They allow for adjustment of only a few variables (see examples in Hudson *et al.*¹²) or otherwise can become convoluted (e.g., Lee *et al.*¹³). In contrast, the use of population PK models allows dose adjustment to be made *a priori* based on any number of covariates (i.e., personalization). The availability of models also enable subsequent optimization of the treatment based on clinical follow-up procedures such as TDM (i.e., individualization) without the need for empirical calculations or drawing lines on graphs by hand. An additional advantage of population PK models is the incorporation of statistical distributions to describe measurement error, which can theoretically lead to more accurate and/or precise parameter estimates depending on the error model; in turn, this results in more accurate dosing recommendations. Moreover, PK models are one of the building blocks of clinical trial simulations, which can provide the basis for the evaluation of alternative dosing scenarios *in silico*.

Here we explore how clinical trial simulations and optimal design concepts can be used to identify suitable dosing algorithms and possibly personalize the treatment of seizures with the available AEDs. It can be anticipated that the implementation of model-based titration and dosing algorithms, as a criterion for dose adjustment and transition to alternative first-line or combination therapy, may prevent treatment failure in a considerable fraction of patients who currently do not respond to the first AED. Our approach may be of particular relevance for the 10–20% of patients who still show unresolved seizures when their target dose has been achieved.³ It may also allow the identification of individuals within the group of patients who would respond to optimized regimens, but currently remain refractory to treatment and are said to have drug-resistant epilepsy.⁴

Finally, we aim to show how TDM procedures can be combined with inferential methods based on modeling and simulation to optimize doses and dosing regimens. These concepts have been increasingly applied to other therapeutic areas (e.g., antitumor,

immunosuppressant, and anti-infective drugs) where favorable treatment outcome depends on the attainment and maintenance of target drug exposure.^{14–18} Such developments illustrate the effective introduction of individualized medicines to patients.¹⁹ This diverges from current clinical practice in epilepsy, which relies on limited clinical evidence and somewhat randomly selected sparse PK sampling when TDM is used. In most cases, blood collection is performed without further understanding of the required number of samples or most appropriate time for collection to ensure accurate estimation of a patient's clearance (CL), which is critical for subsequent dose individualization. So far, no evidence exists on the optimality of such sampling strategies. Typically, optimal sampling is assumed to be at the end of the dosing interval (i.e., trough levels), but this is not always the case (e.g., see details on sampling times between 2–6 h postdose in Yukawa *et al.*²⁰). Moreover, there is often a large spread in sampling times, in part due to factors such as variable dosing time, patient availability, and blood withdrawal service opening times.

For the sake of clarity, here we refer to *personalization* when treatment decisions, including dose adjustment, are based on covariate factors, including demographic, clinical, and pathophysiological data. Such a definition is required to account for the contribution and interaction between multiple factors, other than genotype and phenotype.²¹ We also make use of the term *individualization* to refer to dose adjustments based on TDM and subsequent estimation of the individual patient's PK parameters (e.g., clearance). This distinction is important, as in some cases treatment optimization may be reached without the requirement for TDM. In fact, when used in conjunction with model-based approaches, TDM may form the basis for the individualization of therapy, in particular in special populations such as children and pregnancy.^{22–24}

RESULTS

Implications of dosing algorithms for systemic exposure to AEDs

Although dose levels were found that resulted in concentrations that are within the therapeutic window for 8 out of 11 AEDs in at least 95% of the adult population, large interindividual differences in CL resulted in a wide spread of C_{ss} relative to the target concentration, i.e., RTC_{ss} in the population (**Figure 1**). Personalization improved the precision of RTC_{ss} (CV% of population – CV% of *personalized* scenario) in adults for PHT (see Methods for drug abbreviations) (36.0%) and ZNS (8.5%). No relevant changes (i.e., between –5 to +5%) were found for CBZ, CLBZ, CLNZ, LMT, LVT, OXC, PHB, TPM, and VPA. In children, personalization also improved the precision of RTC_{ss} for PHT (32.9%) and ZNS (5.9%) (**Figure 2**). No relevant differences were found for CBZ, CLBZ, CLNZ, LMT, OXC, PHB, TPM, and VPA. The CV% for the personalization scenario was worse for LVT (–15.6%). Personalization procedures resulted in a reduction of the bias in RTC_{ss} (RE% of population – RE% of *personalized* scenario) for PHT (8.2%), TPM (7.9%), and ZNS (13.5%) in adults, and CLBZ (6.3%), CLNZ (9.4%), OXC (12.8%), and TPM (8.7%) in children. Some bias was observed by personalized dosing of LMT

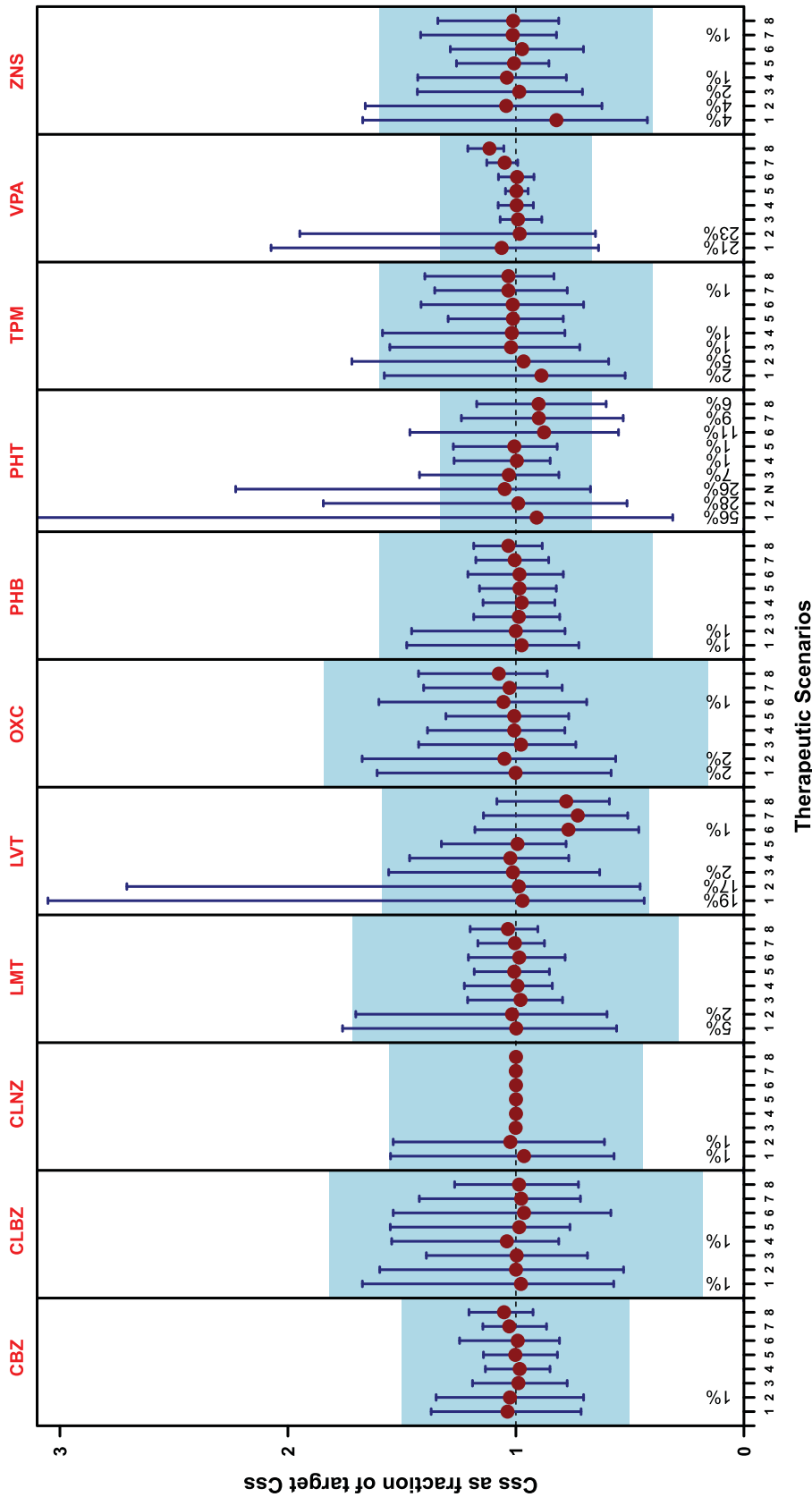


Figure 1 Overview of median (circles) and 95% prediction interval (bars) of drug exposures (C_{ss}) in adults for different drugs and dosing scenarios; therapeutic window shown as a shaded area, numbers listed below the bars are percentages of the population with C_{ss} falling outside the therapeutic window; only values other than 0% are shown. The values of RTC_{ss} at the unity line in the case of clonazepam are probably due to the underlying model parameterization, which does not include absorption and distribution processes. The scenarios shown along the x-axis refer to: 1 = Population; 2 = Personalized; 3 = Individualized based on 1 sample; 4 = Individualized based on 2 samples; 5 = Individualized based on 3 samples; 6 = Individualized based on 1 D-optimized sample; 7 = Individualized based on 2 D-optimized samples; 8 = Individualized based on 3 D-optimized samples. N = Individualized PHT dose based on the nomogram by Ludden et al.⁴⁸ [Color figure can be viewed at cptjournal.com]

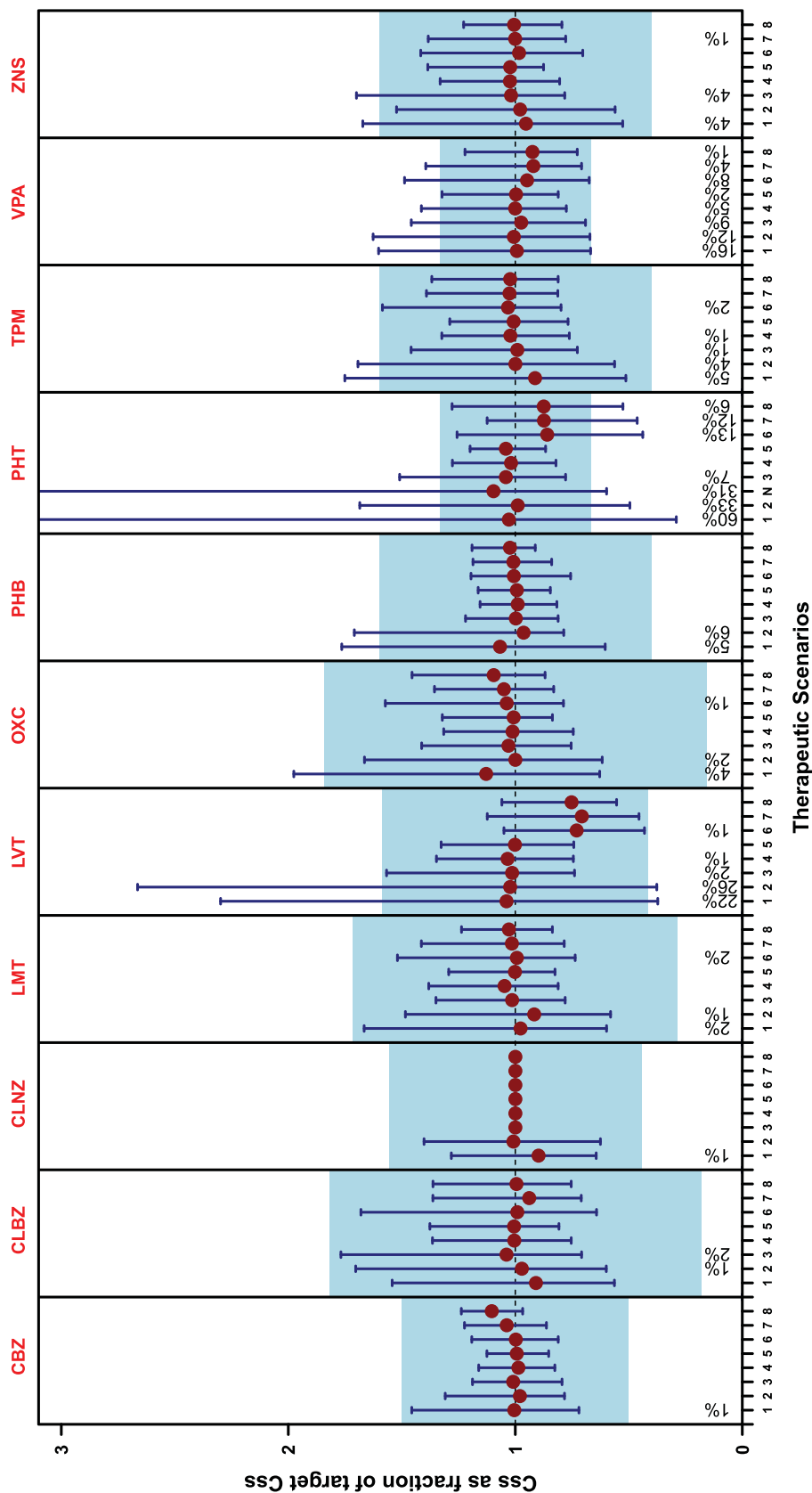


Figure 2 Overview of median (circles) and 95% prediction interval (bars) of drug exposures (C_{ss}) in children for different drugs and dosing scenarios; therapeutic window shown as a shaded area, numbers listed below the bars are percentages of the population with C_{ss} falling outside the therapeutic window; only values other than 0% are shown. The values of RTC_{ss} at the unity line in the case of clonazepam are probably due to the underlying model parameterization, which does not include absorption and distribution processes. The scenarios shown along the x-axis refer to: 1 = Population; 2 = Personalized; 3 = Individualized based on 1 sample; 4 = Individualized based on 2 samples; 5 = Individualized based on 3 samples; 6 = Individualized based on 1 D-optimized sample; 7 = Individualized based on 2 D-optimized samples; 8 = Individualized PHT dose based on the nomogram by Ludden et al.⁴⁸ [Color figure can be viewed at cpt-journal.com]

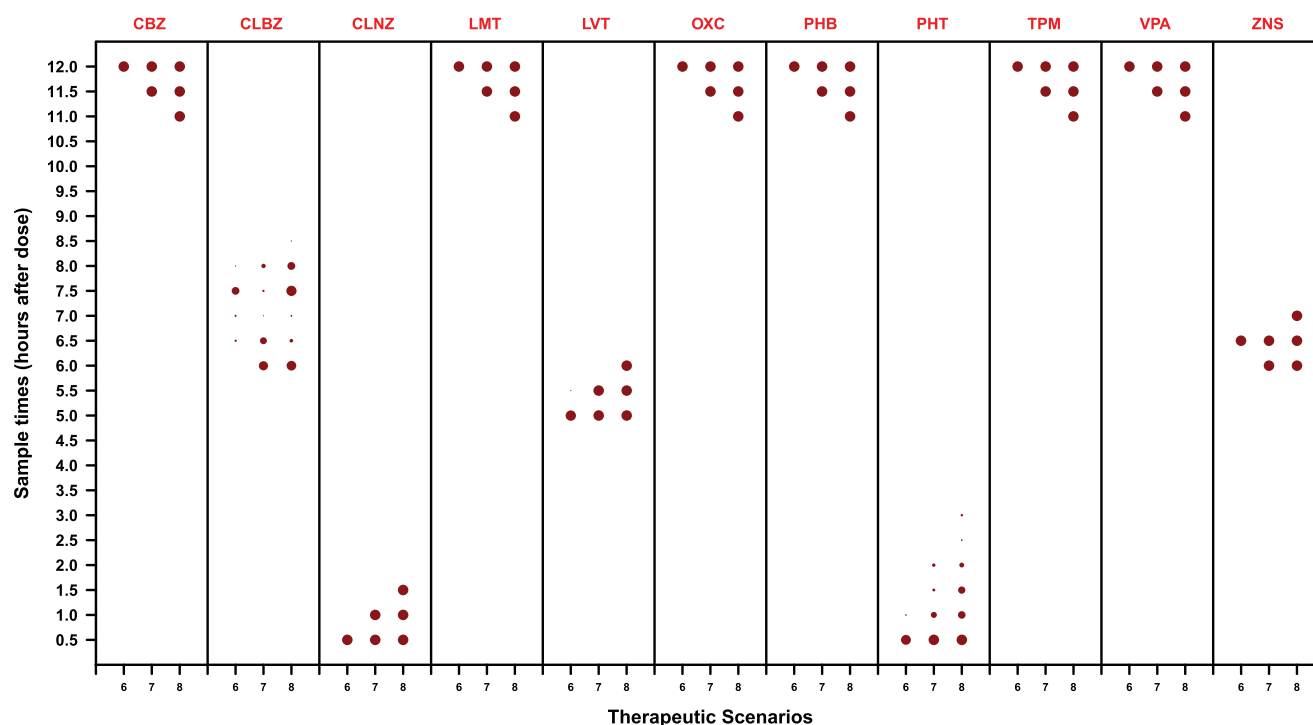


Figure 3 Overview of optimized samples in hours after dose (circles) for each drug and number of samples per individual. The relative size of the circle represents the relative frequency of sampling at each specific timepoint, i.e., if more patients were sampled at the timepoint, a larger circle is depicted. The scenarios shown along the x-axis refer to: 6 = Individualized based on 1 D-optimized sample; 7 = Individualized based on 2 D-optimized samples; 8 = Individualized based on 3 D-optimized samples. [Color figure can be viewed at cpt-journal.com]

(−6.0%) in children. No relevant differences in bias were found for any of the other AEDs.

By contrast, the integration of model-based algorithms with empirical Bayesian estimates (EBE) from TDM using one sample showed improvement in terms of target C_{ss} for nearly all AEDs. Reductions in CV% of RTC_{ss} in adults varied between 6.6% for CBZ and 20.9% for CLBZ. The effect of these procedures was found to be negligible only for TPM (4.6%). In children, similar reductions were observed in CV% of RTC_{ss} , with values varying between 6.0% for CLBZ to 19.9% for CLNZ. Further reductions in the variability of RTC_{ss} could be achieved by evaluating two blood samples instead of one. Such an improvement was observed for LVT (7.5%) in adults and CLBZ (8.4%) in children.

Finally, bias in the RTC_{ss} estimates (RE%) in children could be reduced using one TDM sample only for LMT (6.9%). No improvement in bias was found for any of the other AEDs, irrespective of the number of TDM samples.

Implications of optimized sampling times for TDM

The sampling times for characterization of clearance (trough levels) in adults could be optimized for 6 out of 11 AEDs, whereas for two other compounds, sampling times optimization was achieved by including data relative to the upswing portion of the concentration vs. time curve (Figures 3 and 4). Of note is the fact that optimization procedures show a counterintuitive behavior. When more frequent sampling is required or feasible, one should collect additional samples at timepoints close to the reference sampling times. The spreading of blood samples at

wider intervals such as at 6, 9, and 12 h after dose for once-daily regimens is often less informative than when the additional samples are collected at the end of the dosing interval.

Despite the possibility of introducing optimized times for blood sampling and obtaining increased precision for individual clearance estimates, our findings reveal that such efforts do not ensure improved target attainment. In fact, comparison of CV% of RTC_{ss} between the D-optimized and individualized scenarios (i.e., one vs. one, two vs. two and three vs. three samples) reveals no reductions larger than 5%. By contrast, a worsening was found for PHT in adults (−7.4, −8.5, and −5.1%) and children (−5.4, −6.7, and −9.0%), and LMT (−5.3% for one sample) in children. In addition, bias was not reduced by taking samples at D-optimized sampling times. Surprisingly, D-optimized schemes introduced bias for LVT (−21.7, −24.7, and −21.4%), PHT (−9.2, −9.7, and −9.2%), and VPA (−11.4 when taking three samples) in adults, and for LVT (−25.7, −25.9, and −24.6%), PHT (−9.8, −10.7, and −8.3%), and VPA (−7.9, and −7.3% for two and three samples, respectively).

DISCUSSION

The treatment of epileptic seizures with AEDs is based on the clinical classification of overt seizure type.^{20,21} Whereas heterogeneity in disease is well known and treatment response varies considerably between patients, there has been a long debate about to what extent treatment should be complemented by therapeutic drug monitoring, which is aimed at establishing whether patients

these models were based on sparse data. This may have resulted in an inflated variability in clearance, as often variability in absorption or distribution volume was not included. Consequently, these models may indirectly produce results in favor of the individualized and D-optimized dosing algorithms, as these approaches take into account additional sources of variability, other than clearance. Clearly, given the simplifications, some models may not adequately describe the relevant physiological processes when applied to other conditions or scenarios, such as dosing during nonsteady-state conditions. By contrast, other models may be considered overparameterized. For instance, the models for CLBZ and ZNS incorporate information on genetic polymorphisms for the prediction of clearance, which requires DNA sequencing, a procedure which is not yet commonly used in current clinical practice and may therefore be of limited clinical value. Another example of such limitations is the case of CLNZ, for which the relative target attainment approached unity for the individualized and D-optimized dosing algorithms; the population PK model for this drug does not include interindividual differences in absorption or distribution processes. In real life, some variation would be detected even after integration of the TDM with population PK concepts.

The discrepancies that were found in terms of precision and bias between dose individualization using typical and optimized sampling times may also be due to model limitations, as in the case of LVT and PHT, for which information regarding the underlying correlation between clearance and volume of distribution and variability in the absorption kinetics was missing. A major difference between sampling time optimization in adults and children was seen for LMT and VPA. These differences are most probably caused by the fact that the PK models have been originally developed separately for adults and children. From a statistical perspective, the main difference between the two PK models was the use of additive (adults) and proportional (children) residual errors. When residual error is large and parameterized as proportional-only simulations, they will behave differently from combined error models.

Lastly, we have not limited the dose adjustments to the approved dose ranges or available dosage strengths, as the scope of our investigation was to establish the relevance of model-based principles for the personalization of treatment with AEDs. Nevertheless, we do not anticipate any major differences in the conclusions drawn so far. The predicted doses were within the approved dose ranges even if doses were not adjusted for available strengths.

Current challenges in clinical practice

The implementation of model-based dosing algorithms for individualization of treatment in the clinic is subject to practical, technical, and theoretical challenges, such as the characterization of interindividual differences. As a consequence, historically AED dose adjustments have been restricted to the typical population parameter values, without taking into account the contribution of predefined covariate effects. In fact, exceptions are illustrated by the requirement for dose adjustment in patients with varying degrees of renal and hepatic impairment.

Treatment individualization or precision medicine has become the goal of the clinical research community in other therapeutic areas such as oncology, but its wider acceptance seems to be hindered by limited evidence of its large-scale utility and impact.³¹ Furthermore, the lack of user-friendly software programs over the past decades has imposed the need for technical skills to access and use quantitative technologies. This situation has changed in recent times; advances in computing performance and continuous development of dedicated software packages, such as R and Shiny, have allowed the development of dosing tools with user-friendly graphical user interfaces.³² For example, the use of TDM is popular in antibiotic treatment, and the application TDMx has been created to make use of the available PK models for TDM-based dosing adjustments.³³ Currently, no such software applications exist with the required functionality to integrate bioanalytical results from TDM with a population PK model and patient demographic, clinical, and genetic information to derive individualized dose recommendations for AEDs. Given the availability of dosing algorithms in other fields of medicine, it appears that the lack of such applications for AEDs reflects the entrenched culture in clinical decision making, rather than a technical hurdle. Taking into account the possibility of performing TDM based on a dried blood spot or saliva, it can be anticipated that the implementation of integrated platforms will not represent an increased burden to patient care in epilepsy.^{34,35} A final obstacle for the uptake of TDM-based dosing individualization applications is the lack of standards and consensus regarding the validation requirements for such a platform. At the moment, no clear guidelines exist for such an evaluation. This leads to the use of *ad-hoc* criteria, creating unnecessary complexities and inconsistencies for the development and acceptance of these tools. Agreement on the quality standards and validation requirements may create a more favorable environment for these applications to thrive in. In this respect, the approval of model-based dosing algorithms may require a (regulated) process comparable to what is expected from any diagnostic test or device. One should demonstrate the accuracy and precision of the method as well as the implications of making the “wrong” decision. Public-private partnerships and consortia could play an important role in the development of such standards, acting as custodians and curators.

In summary, some important recommendations arise from our investigation. First, that the use of wide blood sampling intervals for TDM has limited impact on the characterization of individual PK parameters. Second, AED target exposure levels are unlikely to be attained without the use of dosing algorithms and individualized dosing recommendations. Third, available PK models have limitations that highlight the need for standardization and validation procedures. Simplified models can lead to under- or overestimation of variability and thereby to imprecise dosing. On the other hand, models that are too complex may show parameter identifiability issues. In essence, a balance needs to be struck between complexity and usability. The work presented here adds to the increasing evidence that individualized therapy provides an opportunity to prevent failure of treatment with first-line and alternative first-line AEDs, disentangling truly

Table 1 Baseline characteristics of the patient population used across the different simulation scenarios

Demographic	Adult values	Pediatric values
Age range in years (uniformly distributed)	18-65	4-14
Mean, CV% of weight (kg) (normally distributed)	Male: 75, 16% Female: 65, 16%	Age×3+7, ^a 10%
Gender	Male: 50% Female: 50%	Male: 50% Female: 50%

^aBased on the weight-by-age formula proposed by Luscombe and Owens.⁴⁹

drug-resistant patients from those who are labeled as nonresponders, i.e., whose phenotype is a consequence of suboptimal exposure.

METHODS

PK models and virtual patient demographics

Models describing the adult and pediatric PK of carbamazepine (CBZ),³⁶ clobazam (CLBZ),³⁷ clonazepam (CLNZ),²⁰ lamotrigine (LMT),^{38,39} levetiracetam (LVT),⁴⁰ oxcarbazepine (OXC),⁴¹ phenobarbital (PHB),⁴² phenytoin (PHT),⁴³ topiramate (TPM),³⁰ valproic acid (VPA),^{44,45} and zonisamide (ZNS)⁴⁶ were collected from the published literature. Models were transcribed into the appropriate format in R v. 3.1.1,⁴⁷ along with the parameter estimates and combined with analytical solutions of the mathematical equations describing the concentration over time profiles (Eqs. 1 and 2.1–2.5 for one- and two-compartment models, respectively; see online **Supplemental Material** for details).¹² These equations were then implemented as scripts and used for all subsequent simulations. For each AED, separate adult and pediatric populations were evaluated ($n = 1,000$) using the baseline demographic characteristics depicted in **Table 1**. Values of other influential factors, such as genetic polymorphisms, were simulated according to their occurrence as in the original publication. Steady-state concentrations over 12-h dose intervals and C_{ss} (Eq. 3) were simulated for typical adult and pediatric populations (**Table 1**). Hypothetical dosing regimens were considered according to different dosing algorithms (**Table 2**). Steady-state concentrations (C_{ss}) were used as a surrogate marker for AED effect, with the therapeutic target C_{ss} (TC_{ss}) in each scenario set to the concentration halfway between the therapeutic minimum and maximum of the therapeutic window (**Table 3**)¹⁰:

$$C_t = \frac{D}{V} \frac{k_a}{k_a - \frac{CL}{V}} \left(\frac{e^{-\frac{CL}{V}(t-t_D)}}{1 - e^{-\frac{CL}{V}\tau}} - \frac{e^{-k_a(t-t_D)}}{1 - e^{-k_a\tau}} \right) \tag{1}$$

$$\alpha = \frac{Q}{V_2} \frac{CL}{V_1} \tag{2.1}$$

$$\beta = \frac{1}{2} \left(\frac{Q}{V_1} + \frac{Q}{V_2} + \frac{CL}{V_1} - \sqrt{\left(\frac{Q}{V_1} + \frac{Q}{V_2} + \frac{CL}{V_1} \right)^2 - 4 \frac{Q}{V_2} \frac{CL}{V_1}} \right) \tag{2.2}$$

$$A = \frac{k_a}{V_1} \frac{\frac{Q}{V_2} - \alpha}{(k_a - \alpha)(\beta - \alpha)} \tag{2.3}$$

$$B = \frac{k_a}{V_1} \frac{\frac{Q}{V_2} - \beta}{(k_a - \beta)(\alpha - \beta)} \tag{2.4}$$

$$C_t = D \left(\frac{Ae^{-\alpha(t-t_D)}}{1 - e^{-\alpha\tau}} + \frac{Be^{-\beta(t-t_D)}}{1 - e^{-\beta\tau}} - \frac{(A+B)e^{-k_a(t-t_D)}}{1 - e^{-k_a\tau}} \right) \tag{2.5}$$

$$C_{ss} = \frac{F * D * \tau}{CL} \tag{3}$$

$$D_i = \frac{1}{F} * CL_i * TC_{ss,i} * \tau_i \tag{4}$$

where C_t : concentration at time t (mg/L or μ g/L). D : dose (mg or μ g). V or V_1 : central volume of distribution (L). k_a : absorption rate constant (h^{-1}). CL : clearance (L/h). t : time (h). t_D : time of dose (h). τ : dosing interval (h). Q : intercompartmental clearance (L/h). V_2 : peripheral volume of distribution (L). F : bioavailability (fraction of the dose that is absorbed). TC_{ss} : target steady-state concentration (mg/L or μ g/L). i : individual i .

Personalized dosing algorithms

Two different dosing algorithm scenarios were simulated based on the population PK models alone. In an initial scenario, exploratory simulations (not shown) were performed to select one dose for the whole population that resulted in exposures which were the closest to the target exposure in the

Table 2 Model-based dosing algorithms tested in the different scenarios

Dosing algorithm name	Dose calculated using
Standard (population)	Population CL
Personalized	Model-predicted CL, including covariate effects
Individualized (1)	Individual CL prediction based on TDM with 1 sample
Individualized (2)	Individual CL prediction based on TDM with 2 samples
Individualized (3)	Individual CL prediction based on TDM with 3 samples
D-optimized (1)	Individual CL prediction based on TDM with optimized sampling time (1 sample during the elimination phase)
D-optimized (2)	Individual CL prediction based on TDM with optimized sampling times (2 samples during the elimination phase)
D-optimized (3)	Individual CL prediction based on TDM with optimized sampling times (3 samples during the elimination phase)

Table 3 Dose levels simulated for the initial dosing scenario, along with the corresponding therapeutic windows and target steady-state concentration for each drug

Drug	Adult standard dose	Pediatric standard dose	Therapeutic concentration window [9]	Target steady-state concentration
CBZ	700 mg/day	15 mg/kg/day	4-12 mg/L	8 mg/L
CLBZ	20 µg/day	0.4 µg/kg/day	30-300 µg/L	165 µg/L
CLNZ	5 µg/day	0.08 µg/kg/day	20-70 µg/L	45 µg/L
LMT	400 mg/day	7 mg/kg/day	2.5-15 mg/L	8.75 mg/L
LVT	2500 mg/day	50 mg/kg/day	12-46 mg/L	29 mg/L
OXC	1000 mg/day	20 mg/kg/day	3-35 mg/L	19 mg/L
PHB	150 mg/day	4 mg/kg/day	10-40 mg/L	25 mg/L
PHT	300 mg/day	10 mg/kg/day	10-20 mg/L	15 mg/L
TPM	300 mg/day	8 mg/kg/day	5-20 mg/L	12.5 mg/L
VPA	1200 mg/day	20 mg/kg/day	50-100 mg/L	75 mg/L
ZNS	300 mg/day	6 mg/kg/day	10-40 mg/L	25 mg/L

largest proportion of the population. This population scenario was selected as a reference scenario. For subsequent comparisons, there was the assumption that the selected doses reflect the titration procedures used in clinical practice. By contrast, in the personalized dosing scenario, individual clearance estimates were calculated for each patient i (CL_i) using the covariates included in the model. The difference between the initial population dose and personalized dosing scenarios represents the impact of interindividual variability in clearance, which is explained by covariates. Finally, an additional dosing scenario was generated for PHT based on the nomogram of Ludden *et al.*⁴⁸ This nomogram requires two samples at different steady-state doses. We have therefore used 300 and 200 mg/day for adults, and 10 and 6.7 mg/kg/day for children. Based on their nomogram, parameters V_{max} and K_m are calculated and an updated dose can be derived using the formula $V_{max} \cdot TC_{ss} / K_m + TC_{ss}$. It should be noted that the nomogram will derive a negative K_m when higher concentrations are observed for a lower dose as compared to that of the higher dose, in which case their median reported K_m of 7.73 was used instead.

Individualized dosing algorithms

Given that the AEDs are titrated to steady-state conditions, the average plasma concentration at steady state will vary according to the individual patient's clearance (CL). Empirical Bayesian estimation procedures can be used to obtain accurate predictions of the individual parameter of interest. The EBE determines the deviation (η , eta) from the population value (θ , theta) of the parameters of interest (e.g., rate of absorption, volume of distribution, clearance, etc.), taking into account the residual variability (ϵ , epsilon).⁵⁰ Thus, AED concentrations derived from TDM can be used in conjunction with EBE to individualize the dose.^{10,11,51} In theory, such an approach allows one to account for the variability in clearance and other individual PK parameters which are not described by the underlying covariate effects. To date, it is unclear to what degree the proposed dosing algorithm yields higher proportions of patients achieving target C_{ss} (TC_{ss}) when compared to conventional dose adjustment for AEDs based on TDM only.

Here we present three individualized dosing scenarios, in which EBEs were obtained for clearance (CL_i), under the assumption of blood sampling being performed according to empirical sampling schemes, including 1, 2, or 3 samples for each individual patient. When only one sample was collected, sampling was performed at the end of the dosing interval (e.g. 12 h for a b.i.d. regimen) to ensure information about the trough levels. When two samples were used, blood sampling was such that information was obtained about the elimination phase in addition to the trough sample at the end of the dosing interval, i.e., at 9 h and 12 h post-dose. For three samples, data on the elimination phase was obtained at 6,

9, and 12 h postdose. EBEs of clearance were obtained by minimizing the Bayesian objective function:

$$OFV_i = \sum \left(\frac{\bar{Y}_{ij} - Y_{ij}}{\sigma^2} + \ln(\sigma^2) \right) + \sum \left(\frac{\eta_{ik}^2}{\omega_k^2} \right) \quad (5)$$

where \bar{Y}_{ij} is the j^{th} concentration prediction for individual i , Y_{ij} is the j^{th} concentration observed for individual i , σ is the variance of the residual error, η_{ik} is the deviation (eta) from population parameter k in individual i , and ω is the variance of the k^{th} eta. Although EBEs were estimated for all etas, only those for clearance were subsequently used for dose optimization using Eq. 4. The difference between personalized and individualized dosing scenarios reflects the contribution of the parameter distribution describing an additional fraction of the unexplained interindividual variability in clearance. See the online **Supplemental Material** for further details about the optimization of blood sampling for TDM using D-optimal design in software PFIM.

Graphical and statistical summaries of the simulated scenarios

The ratio $RTC_{ss} = C_{ss}/TC_{ss}$ was used to describe how well the C_{ss} resulting from a dosing algorithm compared to the theoretical TC_{ss} . Consequently, values for RTC_{ss} below or above 1 represent underdosing or overdosing, respectively. The observed differences between dosing algorithms for each drug and simulation scenario were graphically analyzed using whisker-box plots of the median and 95% prediction intervals. In addition, the range of PFIM-derived sampling times was used to assess differences in parameter information content for the scenarios involving sampling time optimization. Furthermore, bias and precision of RTC_{ss} were determined by calculating the relative error (RE%) as $(C_{ss} - TC_{ss}) * 100\%$, and coefficient of variance (CV%) as $\text{mean}(RTC_{ss}) / \text{sd}(RTC_{ss}) * 100\%$, respectively. The impact of dosing algorithms on the ability to attain TC_{ss} was determined by taking the difference in CV% and RE% estimates between simulated scenarios.

SUPPLEMENTARY MATERIAL is linked to the online version of the article at <http://www.cpt-journal.com>

ACKNOWLEDGMENT

The research leading to these results received funding from the European Union Seventh Framework Programme FP7/2007-2013 under grant agreement no. 261060.

CONFLICT OF INTEREST

S.C. van Dijkman was funded by FP7 project Global Research in Paediatrics (GRiP). O. Della Pasqua is a member of GRiP and is also Senior Director Clinical Pharmacology at GlaxoSmithkline, UK. The authors have no other relevant affiliations or financial involvement with any organization or entity with a financial interest in or financial conflict with the subject matter or materials discussed in the article apart from those disclosed.

AUTHOR CONTRIBUTIONS

O.D.P. and S.C.v.D. designed the research and wrote the article; S.C.v.D. performed the research; S.C.v.D. and S.W. analyzed the data; O.D.P. and M.D. contributed to the review and discussion of results.

© 2017 The Authors. Clinical Pharmacology & Therapeutics published by Wiley Periodicals, Inc. on behalf of American Society for Clinical Pharmacology and Therapeutics

This is an open access article under the terms of the Creative Commons Attribution-NonCommercial License, which permits use, distribution and reproduction in any medium, provided the original work is properly cited and is not used for commercial purposes.

- van Dijkman, S.C., Alvarez-Jimenez, R., Danhof, M. & Della Pasqua, O. Pharmacotherapy in pediatric epilepsy: from trial and error to rational drug and dose selection — a long way to go. *Expert Opin. Drug Metab. Toxicol.* **12**, 1143–1156 (2016).
- Piana, C., Antunes, N.D.J. & Pasqua, O. Della. Implications of pharmacogenetics for the therapeutic use of antiepileptic drugs. *Expert Opin. Drug Metab. Toxicol.* **10**, 341–358 (2014).
- Kwan, P. & Brodie, M.J. Epilepsy after the first drug fails: substitution or add-on? *Seizure* **9**, 464–468 (2000).
- Dalic, L. & Cook, M.J. Managing drug-resistant epilepsy: challenges and solutions. *Neuroepidemiol. Dis. Treat.* **12**, 2605–2616 (2016).
- van Dijkman, S.C., Rauwé, W.M., Danhof, M. & Della Pasqua, O. Pharmacokinetic interactions and dosing rationale for antiepileptic drugs in adults and children. (Companion paper.)
- Perucca, E. Clinical pharmacokinetics of new-generation antiepileptic drugs at the extremes of age. *Clin. Pharmacokinet.* **45**, 351–363 (2006).
- Italiano, D. & Perucca, E. Clinical pharmacokinetics of new-generation antiepileptic drugs at the extremes of age: an update. *Clin. Pharmacokinet.* **52**, 627–645 (2013).
- Nielsen, J.C. *et al.* Population pharmacokinetics analysis of vigabatrin in adults and children with epilepsy and children with infantile spasms. *Clin. Pharmacokinet.* **53**, 1019–1031 (2014).
- Sugiyama, I., Bouillon, T., Yamaguchi, M., Suzuki, H. & Hirota, T. Population pharmacokinetic analysis for 10-monohydroxy derivative of oxcarbazepine in pediatric epileptic patients shows no difference between Japanese and other ethnicities. *Drug Metab. Pharmacokinet.* **30**, 160–167 (2014).
- Patsalos, P.N. *et al.* Antiepileptic drugs — best practice guidelines for therapeutic drug monitoring: a position paper by the subcommission on therapeutic drug monitoring, ILAE Commission on Therapeutic Strategies. *Epilepsia* **49**, 1239–1276 (2008).
- Neels, H.M. *et al.* Therapeutic drug monitoring of old and newer anti-epileptic drugs. *Clin. Chem. Lab. Med.* **42**, 1228–1255 (2004).
- Hudson, S.A.A., Farquhar, D.L.L., Thompson, D. & Smith, R.G.G. Phenytoin dosage individualisation — five methods compared in the elderly. *J. Clin. Pharm. Ther.* **15**, 25–34 (1990).
- Lee, F.X. *et al.* Developing a nomogram for dose individualization of phenytoin in asian pediatric patients derived from population pharmacokinetic modeling of saturable pharmacokinetic profiles of the drug. *Ther. Drug Monit.* **35**, 54–62 (2013).
- Croes, S., Koop, A.H., Van Gils, S.A. & Neef, C. Efficacy, nephrotoxicity and ototoxicity of aminoglycosides, mathematically modelled for modelling-supported therapeutic drug monitoring. *Eur. J. Pharm. Sci.* **45**, 90–100 (2012).
- Vinks, A.A. The application of population pharmacokinetic modeling to individualized antibiotic therapy. *Int. J. Antimicrob. Agents* **19**, 313–322 (2002).
- Gotta, V. *et al.* Therapeutic drug monitoring of imatinib: Bayesian and alternative methods to predict trough levels. *Clin. Pharmacokinet.* **51**, 187–201 (2012).
- Padulles Caldes, A. *et al.* Optimal sparse sampling for estimating ganciclovir/valganciclovir AUC in solid organ transplant patients using NONMEN. *Ther. Drug Monit.* **36**, 371–377 (2014).
- Brooks, E., Tett, S.E., Isbel, N.M. & Staatz, C.E. Population pharmacokinetic modelling and Bayesian estimation of tacrolimus exposure: Is this clinically useful for dosage prediction yet? *Clin. Pharmacokinet.* **55**, 1295–1335 (2016).
- Cortese, D.A. A vision of individualized medicine in the context of global health. *Clin. Pharmacol. Ther.* **82**, 491–493 (2007).
- Yukawa, E. *et al.* Influence of age and comedication on steady-state clonazepam serum level-dose ratios in Japanese epileptic patients. *J. Clin. Pharmacol. Ther.* **26**, 375–379 (2001).
- Academy of Medical Sciences. Stratified, Personalised or P4 medicine: a new direction for placing the patient at the centre of healthcare and health education (Technical report). May 2015. <<http://www.phgfoundation.org/file/13380>>. Accessed 6 October 2016.
- Borgelt, L.M., Hart, F.M. & Bainbridge, J.L. Epilepsy during pregnancy: focus on management strategies. *Int. J. Womens. Health* **8**, 505–517 (2016).
- Perucca, E., Dulac, O., Shorvon, S. & Tomson, T. Harnessing the clinical potential of antiepileptic drug therapy: dosage optimisation. *CNS Drugs* **15**, 609–621 (2001).
- Jacob, S. & Nair, A.B. An updated overview on therapeutic drug monitoring of recent antiepileptic drugs. *Drugs R D* **16**, 303–316 (2016).
- Jayachandran, D. *et al.* Model-based individualized treatment of chemotherapeutics: Bayesian population modeling and dose optimization. *PLoS One* **10**, 1–24 (2015).
- Van Den Broek, M.P.H. *et al.* Pharmacokinetics and clinical efficacy of phenobarbital in asphyxiated newborns treated with hypothermia. *Clin. Pharmacokinet.* **51**, 671–679 (2012).
- Nakashima, H. *et al.* Determination of the optimal concentration of valproic acid in patients with epilepsy: a population pharmacokinetic-pharmacodynamic analysis. *PLoS One* **10**, e0141266 (2015).
- Ogusu, N. *et al.* Impact of the superoxide dismutase 2 Val16Ala polymorphism on the relationship between valproic acid exposure and elevation of gamma-glutamyltransferase in patients with epilepsy: a population pharmacokinetic-pharmacodynamic analysis. *PLoS One* **9**, e111066 (2014).
- Delattre, M., Savic, R.M., Miller, R., Karlsson, M.O. & Lavielle, M. Analysis of exposure-response of CI-945 in patients with epilepsy: application of novel mixed hidden Markov modeling methodology. *J. Pharmacokinet. Pharmacodyn.* **39**, 263–271 (2012).
- Girgis, I.G. *et al.* Pharmacokinetic-pharmacodynamic assessment of topiramate dosing regimens for children with epilepsy 2 to 10 years of age. *Epilepsia* **51**, 1954–1962 (2010).
- Darwich, A.S. *et al.* Why has model-informed precision dosing not yet become common clinical reality? Lessons from the past and a roadmap for the future. *Clin. Pharmacol. Ther.* Feb 9, (2017).
- Wojciechowski, J., Hopkins, A.M. & Upton, R.N. Interactive pharmacometric applications using R and the Shiny package. *CPT Pharmacometrics Syst. Pharmacol.* **4**, 146–159 (2015).
- Wicha, S.G. *et al.* TDMx: A novel web-based open-access support tool for optimising antimicrobial dosing regimens in clinical routine. *Int. J. Antimicrob. Agents* **45**, 442–444 (2015).
- Milosheska, D., Grabnar, I. & Vovk, T. Dried blood spots for monitoring and individualization of antiepileptic drug treatment. *Eur. J. Pharm. Sci.* **75**, 25–39 (2015).
- Patsalos, P.N. & Berry, D.J. Therapeutic drug monitoring of antiepileptic drugs by use of saliva. *Ther. Drug Monit.* **35**, 5–29 (2013).
- Jiao, Z., Shi, X.-J., Zhao, Z.-G. & Zhong, M.-K. Population pharmacokinetic modeling of steady state clearance of carbamazepine and its epoxide metabolite from sparse routine clinical data. *J. Clin. Pharm. Ther.* **29**, 247–256 (2004).
- Saruwatari, J. *et al.* Effects of CYP2C19 and P450 Oxidoreductase polymorphisms on the population pharmacokinetics of clobazam and N-desmethyloclobazam in Japanese patients with epilepsy. *Ther. Drug Monit.* **450**, 302–309 (2014).
- Rivas, N. *et al.* Population pharmacokinetics of lamotrigine with data from therapeutic drug monitoring in German and Spanish patients with epilepsy. *Ther. Drug Monit.* **30**, 483–489 (2008).

39. He, D. *et al.* Population pharmacokinetics of lamotrigine in Chinese children with epilepsy. *Acta Pharmacol. Sin.* **33**, 1417–1423 (2012).
40. Toublanc, N., Sargentini-Maier, M.L., Lacroix, B., Jacqmin, P. & Stockis, A. Retrospective population pharmacokinetic analysis of levetiracetam in children and adolescents with epilepsy — dosing recommendations. *Clin. Pharmacokinet.* **47**, 333–341 (2008).
41. Park, K.-J. *et al.* Drug interaction and pharmacokinetic modeling of oxcarbazepine in Korean patients with epilepsy. *Clin. Neuropharmacol.* **35**, 40–44 (2012).
42. Goto, S. *et al.* Population estimation of the effects of cytochrome P450 2C9 and 2C19 polymorphisms on phenobarbital clearance in Japanese. *Ther. Drug Monit.* **29**, 118–121 (2007).
43. Odani, A. *et al.* Population pharmacokinetics of phenytoin in Japanese patients with epilepsy: Analysis with a dose-dependent clearance model. *Biol. Pharm. Bull.* **19**, 444–448 (1996).
44. Blanco-serrano, B. *et al.* Population estimation of valproic acid clearance in adult patients using routine clinical pharmacokinetic data. *Biopharm. Drug Dispos.* **20**, 233–240 (1999).
45. Blanco-Serrano, B. *et al.* Valproate population pharmacokinetics in children. *J. Clin. Pharm. Ther.* **24**, 73–80 (1999).
46. Okada, Y. *et al.* Population estimation regarding the effects of cytochrome P450 2C19 and 3A5 polymorphisms on zonisamide clearance. *Ther. Drug Monit.* **30**, 540–543 (2008).
47. R Core Team. *R: A Language and Environment for Statistical Computing* (Vienna, Austria, 2014).
48. Ludden, T. M. *et al.* Individualization of phenytoin dosage regimens. *Clin. Pharmacol. Ther.* **21**, 287–293 (1977).
49. Luscombe, M. & Owens, B. Weight estimation in resuscitation: is the current formula still valid? *Arch. Dis. Child.* **92**, 412–415 (2007).
50. Kang, D., Bae, K.S., Houk, B.E., Savic, R.M. & Karlsson, M.O. Standard error of empirical Bayes estimate in NONMEM VI. *Korean J. Physiol. Pharmacol.* **16**, 97–106 (2012).
51. Bondareva, I.B., Sokolov, A.V., Tischenkova, I.F. & Jelliffe, R.W. Population pharmacokinetic modelling of carbamazepine by using the iterative Bayesian (IT2B) and the nonparametric EM (NPEM) algorithms: implications for dosage. *J. Clin. Pharm. Ther.* **26**, 213–223 (2001).